IL-10 deficiency reveals a role for TLR2-dependent bystander activation of T cells in Lyme arthritis

Sarah K. Whiteside[1], **Jeremy P. Snook**[1], **Ying Ma**[1], **F. Lynn Sonderegger**[1], **Colleen Fisher**[1], **Charisse Petersen**[1], **James F. Zachary**[2], **June L. Round**[1], **Matthew A. Williams**[1], and **Janis J. Weis**[1,*]

[1]Department of Pathology, University of Utah, Salt Lake City, UT, USA

[2]Department of Pathobiology, University of Illinois at Urbana-Champaign, Urbana, IL, USA

Abstract

T cells predominate the immune responses in the synovial fluid of patients with persistent Lyme arthritis; however, their role in Lyme disease remains poorly defined. Using a murine model of persistent Lyme arthritis, we observed that bystander activation of CD4$^+$ and CD8$^+$ T cells leads to arthritis-promoting IFN-γ, similar to the inflammatory environment seen in the synovial tissue of patients with post-treatment Lyme disease (PTLD). T cell receptor (TCR) transgenic mice containing monoclonal specificity towards non-*Borrelia* epitopes confirmed that bystander T cell activation was responsible for disease development. The microbial pattern recognition receptor TLR2 was upregulated on T cells following infection, implicating it as marker of bystander T cell activation. In fact, T cell intrinsic expression of TLR2 contributed to IFN-γ production and arthritis, providing a mechanism for microbial-induced bystander T cell activation during infection. The IL-10 deficient mouse reveals a novel TLR2-intrinsic role for T cells in Lyme arthritis, with potentially broad application to immune pathogenesis.

Introduction

Lyme disease, caused by the tick borne spirochete *Borrelia burgdorferi*, is the most common vector borne illness in North America with estimates of 300,000 cases annually (1). The most common late manifestation of Lyme disease is arthritis, with up to 60% of infected individuals reporting intermittent attacks of joint swelling and pain (2). This can usually be treated successfully with 1–2 months of oral or intravenous antibiotics (1, 3). However, 10–20% of patients present with persistent arthritis for months or years after standard antibiotic regimen, referred to as antibiotic-refractory arthritis or post-treatment Lyme disease (PTLD) (4, 5). Patients are negative for the presence of *B. burgdorferi* DNA after standard antibiotic therapy, raising several questions regarding the etiology of this long-lasting illness (6–8). Persistent Lyme arthritis shares certain pathogenic themes with rheumatoid arthritis such as similar synovial lesions, a dominant T-helper 1 (Th1) CD4$^+$ T cell response in synovial

*Corresponding author: Janis J. Weis, Department of Pathology, University of Utah, 15 North Medical Drive East, Salt Lake City, UT 84112, USA; 801-581-8386; Janis.weis@path.utah.edu.

tissues, and high concentrations of pro-inflammatory chemoattractants for CD4^{+} and CD8^{+} T cells in synovial fluid (9–11).

Several hypotheses have been proposed to explain persistent symptoms following antibiotic treatment including molecular mimicry, dysregulated inflammation, and persistence of bacterial antigens (12–18). Adoptive transfer of CD4^{+} T cells into Rag1-deficient mice, which lack B and T cells, exacerbated the severity of arthritis and suggested a role for dysregulated T cells in Lyme disease (19). More than 8% of the *B. burgdorferi* genome coding sequences are specific for Pam3Cys-modified lipoproteins, which possess the potent ability to stimulate host immune responses by interacting with Toll-like receptor (TLR)1/2 heterodimers (20–24). Experiments with Toll-like receptor 2 (TLR2) whole body knockout mice have demonstrated a compromised host defense and T cell involvement (25–27). Additionally, TLR2 expression on T cells has been shown to act as a costimulatory signal for T cell activation (28–30), and could potentially be playing a role in inappropriate T cell responses during *B. burgdorferi* infection.

There have been numerous reports implicating a variety of CD4^{+} T cells in the pathogenesis of human Lyme disease (31–38). Studies have characterized patients with persistent symptoms as having Th1 CD4^{+} T cells and inflammatory cytokines and chemokines such as IFN-γ, IL-1β IL-6, CXCL9, and CXCL10 present in the synovial fluid, sometimes even months following infection and treatment (31, 32). IL-10$^{-/-}$ mice, which lack the anti-inflammatory mediator IL-10, exhibit transcriptional upregulation of these same inflammatory mediators found in patients, contain CD4^{+} T cells in the joints, and have elevated IFN-γ in the serum at 2 weeks post-infection despite extremely low levels of *B. burgdorferi* in the joint tissue (39, 40). The absence of IL-10 exposes the pathogenic potential of T cells whose activation threshold has been lowered during *B. burgdorferi* infection. We have utilized the IL-10$^{-/-}$ mouse as a model for persistent Lyme arthritis to further investigate the arthritis-promoting properties of CD4^{+} T cells and IFN-γ in response to *B. burgdorferi* infection.

Despite correlative evidence linking aberrant T cell responses to other inflammatory arthritis diseases such as rheumatoid arthritis (41), the role of dysregulated T cell responses in the development of persistent Lyme arthritis has yet to be elucidated. In the current study, we show that activation of either CD4^{+} or CD8^{+} T cells is required for the development of Lyme arthritis, which persists in the presence of extremely low levels of *B. burgdorferi* antigen. Using transgenic mouse models, we demonstrate T cell activation occurs independent of *Borrelia*-specific TCR interaction. Furthermore, we show that *B. burgdorferi* infection increases TLR2 expression on T cells. Cell transfer experiments revealed TLR2 as a critical mediator of T cell activation following *B. burgdorferi* infection, which results in enhanced IFN-γ production and Lyme arthritis. These results identify a novel mechanism of Lyme arthritis development dependent on TLR2 bystander activation of CD4^{+} and CD8^{+} T cells.

Materials and Methods

Experimental Animals

C57BL/6, C57BL/6 IL-10$^{-/-}$ (B6.129P2-$Il10^{tm1Cgn}$/J), C57BL/6 TCRα$^{-/-}$ (B6.129S2-$Tcra^{tm1Mom}$/J), C57BL/6 Rag1$^{-/-}$ (B6.129S7-$Rag1^{tm1Mom}$/J), and C57BL/6 TLR2$^{-/-}$ (B6.129-$Tlr2^{tm1Kir}$/J) mice were obtained from Jackson Laboratories. C57BL/6 Rag2$^{-/-}$/OT-I mice were purchased from Taconic. SMARTA TCR transgenic mice, specific for the immunodominant Class-II-restricted epitope of lymphocytic choriomeningitis virus (LCMV) Glycoprotein, GP$_{61-80}$ (42), were maintained on a C57BL/6 background and additionally crossed to IL-10$^{-/-}$ mice (SMARTA/IL-10$^{-/-}$ mice). SMARTA/IL-10$^{-/-}$ mice were further crossed to TCRα$^{-/-}$ mice. Rag2$^{-/-}$/OT-I mice were crossed to IL-10$^{-/-}$ mice. Genotyping was performed according to protocol provided by The Jackson Laboratory for the IL-10 and TCRα mutation. Experiments were performed using mice 5–7 weeks of age, with male and female mice equally distributed into experiment and control groups. In order to prevent colitis development, IL-10$^{-/-}$, SMARTA/TCRα$^{-/-}$/IL-10$^{-/-}$, and OT-I/Rag2$^{-/-}$/IL-10$^{-/-}$ mice were kept on antibiotic water (trimethoprim and sulfamethoxazole) until one day prior to infection. Mouse colonies were housed in the pathogen-free facility at the University of Utah. All mice used in this study were cared for in accordance with the guidelines of the Institutional Animal Care and Use Committee (IACUC) of the National Institutes of Health, and all animal experiments were approved by the IACUC.

Bacteria strain and infection of mice

The N40 isolate of *B. burgdorferi* (provided by S. Barthold, University of California, Davis, CA) was grown to late log phase in Barbour-Stoenner-Kelly (BSK)-II medium supplemented with 6% rabbit serum (Sigma Aldrich). Mice were infected with 2×10^4 *B. burgdorferi* by intradermal injection into the skin of the back. Infection was confirmed in mice sacrificed at one and two weeks by the culture of *B. burgdorferi* from the bladder as described (25). ELISA quantification of *B. burgdorferi*-specific IgM and IgG concentrations were used to confirm infection in mice sacrificed at and after 14 days of infection as previously published (25). To measure *in vivo* cytokine production, mice were injected intravenously with 0.25 mg Brefeldin A (Sigma-Aldrich) in PBS 6 hours before sacrifice (43).

Assessment of Arthritis Severity

Ankle measurements were obtained using a metric caliper before and four weeks post-infection by an investigator blinded to the experimental group. Rear ankle joints were prepared for assessment of histopathologic lesions by removal of the skin and tissue was fixed in 10% neutral buffered formalin. Joints were decalcified and embedded in paraffin, sectioned at 3 μm, and stained with H&E. Lesions were scored in a blinded fashion, with each slide receiving a score of 0–5 for the characteristics of the disease such as polymorphonuclear leukocyte (PMN) and mononuclear cell (lymphocytes, monocytes, macrophages) infiltration into inflammatory processes, tendon sheath thickening (hypertrophy and hyperplasia of surface cells and/or underlying dense sheets of cells resembling immature fibroblasts, synoviocytes, and/or granulation tissue), reactive/reparative responses (periosteal hyperplasia and new bone formation and remodeling), and overall lesion (composite score based on all lesions observed in 6–8 sections per joint), with

5 representing the most severe lesion, and 0 representing no lesion as previously described (44).

Injection of Monoclonal Antibodies

Antibodies used in neutralized or depletion studies were purchased from Bio X Cell and were aggregate and endotoxin free, and sterile. Cellular subsets were depleted by administering 0.2 mg of antibody into the intraperitoneal cavity every 4 days beginning 1 day prior to infection as indicated: anti-CD4 (GK1.5), anti-CD8 (YTS 169.4). Rat IgG2b (LTF-2) was used as the isotype control. IFN-γ was neutralized using 1 mg of anti-IFN-γ (XMG1.2) 1 day prior to infection, followed by additional doses of 0.5 mg anti-IFN-γ every 4 to 5 days. Rat IgG1 (HRPN) was used as the isotype control for IFN-γ neutralization. Cellular depletions of $CD4^+$ and $CD8^+$ T cells were confirmed by flow cytometry (Figure S2).

Intracellular staining, restimulation, and isolation of T cells

$CD3^+CD4^+$ and $CD3^+CD8^+$ T cells were isolated from popliteal and inguinal lymph nodes for intracellular cytokine staining. For mice treated with Brefeldin A, 1×10^6 cells were stained with surface markers and incubated for 30 min at 4°C. Cells were fixed/permeabilized in 100 μl Cytofix/Cytoperm (BD Bioscience). Cells were resuspended in 100 μl Perm/Wash buffer with fluorochrome-conjugated IFN-γ, briefly vortexed, and incubated on ice in the dark for 45 mins. Cells were resuspended in 200 μl PBS + 2% FBS for analysis by flow cytometry. Restimulation of $IL-10^{-/-}$ (Figure 1A and 1B, Figure 3C), SMARTA/$TCR\alpha^{-/-}/IL-10^{-/-}$ (Figure 4E), and OT-I/$Rag2^{-/-}/IL-10^{-/-}$ (Figure 5D) cells was performed for 4 hours with 20 ng/mL PMA and 1 μM ionomycin at 37° C in the presence of Brefeldin A (GolgiPlug, 1μl/mL). For cell transfer experiments (Figure 7), $CD3^+CD4^+$ and $CD3^+CD8^+$ T cells were isolated from lymph nodes (popliteal and inguinal) and spleens of WT C57BL/6 and $TLR2^{-/-}$ mice using the Pan T Cell Isolation Kit II (Miltenyi Biotec). T cell sorting purity was determined by flow cytometry.

Phosphorylation of ZAP-70

Splenocytes from naïve SMARTA/$TCR\alpha^{-/-}/IL-10^{-/-}$ and OT-I/$Rag2^{-/-}/IL-10^{-/-}$ were isolated and 1×10^6 cells were stimulated for 3 hours at 37° C in the presence of 1μM GP_{61-80} peptide (GLKGPDIYKGVYQFKSVEFD), 1μM $Ova_{257-264}$ peptide (SIINFEKL), or 5 μg/mL of sonicated *B. burgdorferi*. Unstimulated cells incubated with media alone were used as a control. After stimulation, cells were fixed in 100 μl of 37° C 1.5% paraformaldehyde (PFA) and incubated at 37° C for 10 minutes. After fixation, cells were stained with surface markers CD4, CD8 and Vα2 in PBS containing 2% FBS for 25 minutes on ice in the dark. Cells were permeabilized using 100 μl of cold 100% methanol for 10 minutes on ice. Cells were centrifuged and resuspended in 100 μl of PBS containing 2% FBS with pZAP-70/SYK (Y319/Y352) clone n3kobu5 (eBioscience™) and incubated on ice in the dark for 45 minutes. Total ZAP-70 clone 1E7.2 (eBioscience™) was used as a control. ZAP-70 Phosphorylation was analyzed using flow cytometry.

Isolation of RNA and quantitative RT-PCR

RNA was purified from the tibiotarsal joints after the skin had been removed. Tissue was immediately immersed in RNA stabilization solution (Invitrogen) and stored at −80°C. Total RNA was recovered from homogenized tissue using the Direct-zol™ kit (Zymo Research). RNA recovered from tissue and cells was reverse transcribed, and transcripts were quantified using a Roche LC-480 qRT-PCR machine according to our previously described protocols (Crandall 2006). Primer sequences used in this study were as follows: *CD8β* (CD8) FWD (5'-CTCTGGCTGGTCTTCAGTATGA-3') REV (5'-TCTTTGCCGTATGGTTGGTTT-3'), *TLR2* FWD (5'-TTGAAGAACTCAGCCTGTAAG-3') REV (5'-GCTTCCAGAGTCTCCAGTTTG-3') Primer sequences for *B. burgdorferi 16S rRNA* (45), *β-actin*, (46) *CD4* (39), *Ifng, Cxcl9* (47), *and Cxcl10* (39), can be found in the indicated citations.

Flow Cytometry

Flow cytometry data were collected on a LSR Fortessa (BD Biosciences) flow cytometer and analyzed using FlowJo (v.10) software. FACS cell sorting was performed using FACSAria (BD Biosciences). Confirmation of cell sorting efficiency was performed using qRT-PCR. Cell surface stains were done in PBS containing 2% FBS. Intracellular stains for cytokines were done using a kit per manufacturer's instructions (BD Biosciences). Position of gates for sorting and analysis was based on analysis of appropriate isotype controls. Fluorochrome-conjugated antibodies from BioLegend were: CD3ε, CD4, CD8α, CD19, CD44, CD62L, IFN-γ, NK1.1, and and Vα2. Fluorochrome-conjugated antibodies from eBioscience™ were: TLR2 and pZAP-70.

Enzyme-linked immunosorbent assay (ELISA) analysis of mouse serum

Blood was obtained from the tail vein of mice 2 weeks post-infection and collected by submandibular puncture at the time of sacrifice. Serum was isolated and stored at −20° C prior to analysis. IFN-γ concentration in serum samples were detected by sandwich ELISA using clone R4-6A2 as the capture antibody, and biotinylated antibody (XMG1.2) for detection. In order to determine *B. burgdorferi*-specific IgM and IgG concentrations, microtiter plates were coated with either sonicated *B. burgdorferi* or goat antibody (Ab) to mouse IgG and IgM (Life Technologies). Serum dilutions were added to plates for 90 min at 37°C and bound murine Ig was detected by addition of HRP-conjugated Abs to murine IgG or IgM (Thermo Fisher Scientific). Ig content was estimated by comparing with standard curves using purified IgG or IgM as previously described (25).

Quantification and Statistical Analysis

The number of mice per group is annotated in corresponding figure legends. Statistical analysis was performed using Prism 6.0d software. Multiple-sample data sets were analyzed by one-way ANOVA followed by Bonferroni's post-hoc test for pair-wise comparisons, as appropriate and indicated in figure legends. Two-sample data sets were analyzed by Student *t* test. Categorical data for histopathology was assessed by Mann-Whitney *U* test. In all figures, data represent the mean ± the stranded error of the mean (SEM). P values correlate

with symbols as follows: ns = not significant, * p   0.05, ** p   0.01, *** p   0.001, **** p
0.0001.

Results

Lyme Arthritis is persistent and sustained in the absence of IL-10

The involvement of CD4^{+} T cells in the pathogenesis of human Lyme disease is seen even
months following infection (9, 10), prompting investigation of a model that would allow
assessment of the contribution of T cells. We have shown previously that the mild arthritis in
C57BL/6 mice is increased in the absence of IL-10 despite greatly reduced numbers of *B.
burgdorferi* in the joint tissue (39, 48). To determine if C57BL/6 IL-10$^{-/-}$ mice could be
used as a model of the persistent Lyme arthritis seen in human patients, infected mice were
followed for 18 weeks. *B. burgdorferi* 16s rRNA was no longer detectable in the joint tissue
of IL-10$^{-/-}$ mice at this time (Table 1). In addition, IL-10$^{-/-}$ mice displayed sustained
upregulation *Ifng*, *Cxcl9*, and *Cxcl10* transcripts in the joint tissue (Table 1), similar to
observations in the synovial fluid of human patients months following antibiotic therapy (49,
50). In contrast, arthritis-resistant wild-type C57BL/B6 mice continued to harbor detectable
amounts of *B. burgdorferi* 18 weeks after infection; however, *Ifng*, *Cxcl9*, and *Cxcl10*
transcripts were not upregulated in the joint tissue (Table 1). These results suggest that
IL-10$^{-/-}$ mice are a suitable model for the investigation of the arthritis-promoting properties
of CD4^{+} T cells and IFN-γ in *B. burgdorferi* infection, as seen in human patients. This has
not been possible in the widely studied C3H mouse, where neither T cells nor IFN-γ are
required for arthritis development (47, 51, 52).

CD4^{+} and CD8^{+} T cells from B. burgdorferi-infected mice produce IFN-γ: ex vivo analysis

Localized IFN-γ production has been observed in the synovial fluid of patients with
persistent symptoms (53). Similarly, arthritis development in IL-10$^{-/-}$ mice is dependent on
both systemic and localized production of IFN-γ (39). Canonical sources of IFN-γ include
Th1 CD4^{+} T cells, natural killer (NK) cells, and NKT cells, all of which are found in the
joint tissue of *B. burgdorferi* infected IL-10$^{-/-}$ mice (39, 54). To define the cellular sources
of IFN-γ in Lyme arthritis development, IL-10$^{-/-}$ mice were infected with *B. burgdorferi*
and cells were harvested from the draining popliteal and inguinal lymph nodes 4 weeks post-
infection which is the peak of arthritis severity. Cells were restimulated in the presence of
phorbol myristate acetate (PMA) and ionomycin for 4 hours and then intracellularly stained
for IFN-γ and analyzed by flow cytometry. This allowed for the identification of cells poised
to produce IFN-γ. The frequency of both CD4^{+}IFN-γ^{+} and CD8^{+}IFN-γ^{+} T cells was
increased compared to mock-infected mice (Figure 1A). IFN-γ was not produced by NK or
NKT cells in response to PMA/ionomycin stimulation (data not shown), thus suggesting that
the majority of IFN-γ producing cells were T cells. The production of IFN-γ is specific to
the draining lymph nodes, as T cells do not produce IFN-γ in other secondary lymphoid
organs such as the spleen (data not shown). These proportional increases in IFN-γ^{+}
lymphocyte populations were also reflected in total cell numbers (Figure 1B). Furthermore,
CD4^{+} and CD8^{+} T cells were producing more IFN-γ on a per cell basis compared to
controls (Figure 1B). Interestingly, although there were fewer IFN-γ^{+} producing CD4^{+} T
cells than CD8^{+} T cells, CD4^{+} T cells were secreting more IFN-γ than CD8^{+} T cells as

measured by mean fluorescence intensity (MFI). Together, these data suggest that both CD4$^+$ and CD8$^+$ T cells are poised to make IFN-γ following *B. burgdorferi* infection.

CD4$^+$ and CD8$^+$ T cells produce IFN-γ in vivo throughout B. burgdorferi infection

In order to capture the actual *in vivo* cytokine production during the course of *B. burgdorferi* infection, infected IL-10$^{-/-}$ mice were injected intravenously with the Golgi blocking agent, Brefeldin A, six hours prior to sacrifice (43). CD4$^+$ and CD8$^+$ T cells were analyzed for activation and functional markers by flow cytometry. Intracellular staining revealed an increase in the frequency and number of CD4$^+$ and CD8$^+$ T cells producing IFN-γ throughout infection (Figure 1C and 1D). Importantly, the number of both CD4$^+$IFN-γ^+ and CD8$^+$IFN-γ^+ T cell were equivalent by 4 weeks post-infection, demonstrating that both are playing a critical role in IFN-γ production (Figure 1D). At 4 weeks post-infection, during peak arthritis severity, both CD4$^+$ and CD8$^+$ T cells had expanded roughly 3-fold, suggesting that both CD4$^+$ and CD8$^+$ are either trafficking to or proliferating in the draining lymph nodes during arthritis development (Figure S1A and S1B). CD44 expression was assessed as an additional indicator of T cell activation status. Both the frequency and total number of CD4$^+$CD44^{hi} and CD8$^+$CD44^{hi} T cells increased throughout infection, demonstrating that *B. burgdorferi* induces activation of both CD4$^+$ and CD8$^+$ T cells (Figure 1E and 1F). Together these data indicate that CD4$^+$ and CD8$^+$ T cells are expanding in the draining lymph nodes upon *B. burgdorferi* infection and they are functionally active as demonstrated through increased IFN-γ production and CD44 expression.

Both CD4$^+$ and CD8$^+$ T cells contribute to the development of Lyme arthritis

Since CD4$^+$ and CD8$^+$ T cells are the primary cellular sources of IFN-γ in the draining lymph nodes, we hypothesized that they were both necessary and sufficient for the development of Lyme arthritis in IL-10$^{-/-}$ mice following *B. burgdorferi* infection. To directly assess the contribution of CD4$^+$ and CD8$^+$ T cells, *B. burgdorferi* infected IL-10$^{-/-}$ mice were treated with depleting antibodies directed towards CD4, CD8, or a combination of both throughout infection (**Methods**). Depletion efficiency was measured throughout the length of the experiment by flow cytometric analysis of blood, and also analyzed at the time of sacrifice in the draining lymph nodes and the joints and determined to be greater than 95% effective (Figure S2A–S2C). Arthritis severity in mice receiving anti-CD4 antibody was similar to mice receiving isotype control, whereas neutralization of CD8 partially reduced arthritis (Figure 2A). The neutralization of both CD4 and CD8 reduced ankle swelling and histopathology scores (Figure 2A and 2B). Mice that were treated with anti-CD4 displayed an increase in bacterial burden in joint tissue as compared to isotype control treated animals (Figure 2C), which is consistent with previous studies (55). Interestingly, CD4$^+$ T cells play a role in host defense not shared by CD8$^+$ T cells as mice treated with anti-CD8 did not display an increase in bacterial burden in joint tissue (Figure 2C). *B. burgdorferi*-infected IL-10$^{-/-}$ mice expressed transcripts for *Ifng, Cxcl9*, and *Cxcl10* in joint tissue which was significantly reduced only in mice treated with a combination of anti-CD4 and anti-CD8 (Figure 3D–3F). These data indicate that both CD4$^+$ and CD8$^+$ T cells contribute the expression of IFN-γ and IFN-γ-dependent genes in the joints of *B. burgdorferi* infected mice. In the absence of CD4$^+$ T cells, the number of CD8$^+$IFN-γ^+ T cells increased substantially, suggesting that CD8$^+$ T cells are able to compensate for the

loss of CD4$^+$-derived IFN-γ (Figure S2D). The number of CD4$^+$IFN-γ^+ T cells also increased in the absence of CD8$^+$ T cells. Taken together, these data demonstrate that CD4$^+$ and CD8$^+$ T cells act synergistically to drive Lyme arthritis. These findings additionally highlight the lack of correlation between the bacterial burden of *B. burgdorferi* and the development of arthritis.

B. burgdorferi infection results in universal expansion and activation of CD4$^+$ and CD8$^+$ T cells

We next explored the possibility that T cells were being activated in a manner independent of classical T cell receptor (TCR)-mediated recognition. In order to address this possibility, the relative distribution of 14 different T cell receptor beta-chain variable regions (TCR-Vβ's) subsets were examined in T cells from draining lymph nodes of *B. burgdorferi* infected IL-10$^{-/-}$ mice using a TCR Vβ repertoire panel (BD Bioscience). TCR Vβ profiling is a standard assay routinely used in our lab (56, 57), and antigen-specific T cell activation results in population skewing towards a few select TCR Vβ families. Stimulation of WT C57BL/6 lymph node cells with the immunodominant Glycoprotein, GP$_{61-80}$, from lymphocytic choriomeningitis virus (LCMV) results in expansion of TCR Vβ 8.3 (data not shown). In contrast, bystander T cell responses involve a wide diversity of TCRs, suggesting antigen-independent activation (58). IL-10$^{-/-}$ mice displayed increased numbers of CD4$^+$ and CD8$^+$ T cells in the draining lymph nodes during *B. burgdorferi* infection (Figure 3A and Figure S1A and S1B). However, there was no selective expansion of any individual Vβ subset on either CD4$^+$ or CD8$^+$ T cells during *B. burgdorferi* infection which is indicative of a polyclonal or non-specific T cell response. (Figure 3B and 3C). Similarly, we did not observe any change in the frequency of IFN-γ producing cells among TCR Vβ subsets following infection (Figure 3C). These results support the hypothesis that T cell expansion in the draining lymph nodes during *B. burgdorferi* infection is independent of antigen-specificity.

B. burgdorferi infection results in antigen-independent expansion and activation of TCR transgenic CD4$^+$ T cells

In order to directly confirm antigen-independent activation of CD4$^+$ T cells, TCR transgenic SMARTA mice were used. SMARTA mice possess CD4$^+$ T cells with monoclonal specificity for the MHC Class II-restricted epitope of lymphocytic choriomeningitis virus (LCMV) glycoprotein, GP$_{61-80}$. This epitope is not found in *B. burgdorferi*, thus SMARTA CD4$^+$ T cells cannot not become activated through TCR engagement during *B. burgdorferi* infection. In order to determine if antigen-independent activation was occurring during *B. burgdorferi* infection, SMARTA mice were crossed to IL-10$^{-/-}$ mice to generate TCR transgenic SMARTA/IL-10$^{-/-}$ mice (**Methods**). To further eliminate the possibility that residual non-SMARTA T cell receptors (present on approximately 5% of T cells) or dual T cell receptors on SMARTA T cells could recognize *B. burgdorferi* antigens, the SMARTA/IL-10$^{-/-}$ mice were further crossed to a TCR$\alpha^{-/-}$ background (SMARTA/TCR$\alpha^{-/-}$/IL-10$^{-/-}$).

SMARTA/TCR$\alpha^{-/-}$/IL-10$^{-/-}$ mice and IL-10$^{-/-}$ were infected with *B. burgdorferi* and sacrificed 4 weeks post-infection. SMARTA/TCR$\alpha^{-/-}$/IL-10$^{-/-}$ mice developed severe

arthritis and histopathologic lesions, suggesting that *B. burgdorferi*-specific T cells are not responsible for arthritis development (Figure 4A–B). Further histopathologic analysis of infected SMARTA/TCRα$^{-/-}$/IL-10$^{-/-}$ mice revealed that the tendon sheath (ts) is reactive and thickened. Synoviocytes (arrowheads) covering the tendon and lining the tendon sheath are reactive and increased in number and size. Adjacent supporting stroma (extracellular matrix [ECM]) under the tendon sheath is also thickened and contains neutrophils (subacute inflammation) admixed with lymphocytes and occasional macrophages (i.e., mononuclear inflammatory cells) as well as immature fibroblasts and collagen fibers (Figure 4B). Examination of the draining lymph nodes from *B. burgdorferi*-infected SMARTA/TCRα$^{-/-}$/IL-10$^{-/-}$ mice revealed an increase in CD4$^+$ T cells compared to mock-infected controls, indicating expansion of TCR transgenic T cells (Figure 4D). In addition, the number of CD4$^+$IFN-γ$^+$ T cells increased in *B. burgdorferi*-infected SMARTA/TCRα$^{-/-}$/IL-10$^{-/-}$, indicating that classical TCR recognition of *B. burgdorferi* antigen is not required for IFN-γ secretion by CD4$^+$ T cells (Figure 4E). Concentrations of *B. burgdorferi* 16S rRNA were observed in the joint tissue of SMARTA/TCRα$^{-/-}$/IL-10$^{-/-}$ mice (Figure 4F). Joint tissue was also analyzed for the presence of *Ifng*, *Cxcl9*, and *Cxcl10* transcripts, all of which were elevated in infected SMARTA/TCRα$^{-/-}$/IL-10$^{-/-}$ mice compared to mock-infected controls (Figure 4G–I). We observed an increase in *B. burgdorferi*-specific IgM and a decrease in *B. burgdorferi*-specific IgG in infected SMARTA/TCRα$^{-/-}$/IL-10$^{-/-}$ mice compared to IL-10$^{-/-}$ mice (Figure 4J and 4K), suggesting there is a lack of T cell help for class switching. In order to confirm that there were no cross-reactive antigens present in *B. burgdorferi*, phosphorylation of the direct substrate of TCR activation, ZAP-70, was assayed. SMARTA/TCRα$^{-/-}$/IL-10$^{-/-}$CD4$^+$ T cells displayed increased phosphorylation of ZAP-70 when stimulated with their cognate antigen, GP$_{61-80}$. However, when stimulated with *B. burgdorferi*, there was no phosphorylation of ZAP-70, indicating that TCR signaling is not occurring (Figure 4L). It has been previously shown that neutralization of IFN-γ in infected IL-10$^{-/-}$ mice significantly reduced ankle swelling and histopathology scores (39). IFN-γ-neutralization in infected SMARTA/TCRα$^{-/-}$/IL-10$^{-/-}$ mice also resulted in a significant decrease in arthritis severity and histopathology scores (Figure S3A and S3B). However, arthritis was still elevated above mock infected animals indicating other components are also contributing to arthritis. Interestingly, IFN-γ-neutralization did not affect expansion of SMARTA/TCRα$^{-/-}$/IL-10$^{-/-}$ CD4$^+$ T cells in the draining lymph nodes (Figure S3C) but resulted in decreased expression of *Ifng, Cxcl9, and Cxcl10* in joint tissue, providing further support that IFN-γ influences arthritis development upon *B. burgdorferi* infection in CD4$^+$ transgenic mice (Figure S3E–G). Overall, these data demonstrate that *B. burgdorferi* infection results in antigen-independent expansion and activation of CD4$^+$ T cells in the draining lymph node resulting in the development of arthritis.

B. burgdorferi infection of CD8$^+$ TCR transgenic mice results in arthritis and IFN-γ production

In order to determine if CD8$^+$ T cells were contributing to the development of Lyme arthritis in an antigen-independent mechanism, TCR transgenic Rag2$^{-/-}$/OT-I mice were used. Rag2$^{-/-}$/OT-I mice possess CD8$^+$ T cells with monoclonal specificity to chicken ovalbumin-derived MHC Class I-restricted epitope Ova$_{257-264}$. Rag2$^{-/-}$/OT-I mice were crossed to IL-10$^{-/-}$ mice to generate OT-I/Rag2$^{-/-}$/IL-10$^{-/-}$ mice. OT-I/Rag2$^{-/-}$/IL-10$^{-/-}$ and IL-10$^{-/-}$

mice were infected with *B. burgdorferi* and sacrificed 4 weeks post-infection. OT-I/Rag2$^{-/-}$/IL-10$^{-/-}$ mice developed severe arthritis and histopathologic lesions similar to IL-10$^{-/-}$ mice (Figure 5A and 5B). Examination of the draining lymph nodes revealed a trending increase in CD8$^+$ T cells from OT-I/Rag2$^{-/-}$/IL-10$^{-/-}$ mice compared mock-infected controls (Figure 5C), similar to CD8$^+$ T cells in the IL-10$^{-/-}$ experimental group included for comparison (Figure 5C). In addition, there was a trending increase in CD8$^+$IFN-γ$^+$ T cells in the lymph nodes of OT-I/Rag2$^{-/-}$/IL-10$^{-/-}$ compared to mock-infected controls, indicating that CD8$^+$ T cells are capable of producing IFN-γ following Borrelia-induced bystander activation (Figure 5D). We observed concentrations of *B. burgdorferi* 16S rRNA in the joints of OT-I/Rag2$^{-/-}$/IL-10$^{-/-}$ mice, likely due to the absence of B cells (Figure 5E). There was also a similar type II interferon profile observed in joint tissues as *Ifng*, *Cxcl9*, and *Cxcl10* transcripts were all elevated in *B. burgdorferi*-infected OT-I/Rag2$^{-/-}$/IL-10$^{-/-}$ mice as compared to mock-infected controls (Figure 5F–5H). The use of a second TCR transgenic mouse which consists of CD8$^+$ T cells recognizing a different antigen (ovalbumin) further addresses the unlikely possibility of a cross-reactive Borrelia epitope. Phosphorylation of ZAP-70 did not occur when OT-I CD8$^+$ T cells were stimulated with *B. burgdorferi*, indicating that T cell activation was not occurring through the TCR (Figure 5I). Similar to the observations made for CD4$^+$ T cells, these results indicate that CD8$^+$ T cell activation and IFN-γ production occurs via bystander activation during *B. burgdorferi*-induced arthritis. Overall, our results indicate a critical role for bystander T cell activation in mediating IFN-γ-dependent Lyme arthritis.

Lyme arthritis results in increased transcription and expression of TLR2 on CD4$^+$ and CD8$^+$ T cells

B. burgdorferi possess lipoproteins with a potent ability to stimulate host pathogen recognition receptors such as TLRs. TLR2 has been implicated as an important player in host defense, as TLR2$^{-/-}$ mice experience deficiencies in clearing *B. burgdorferi* and harbor more bacteria in the joints compared to wild-type mice (25, 26). It has recently been appreciated that both CD4$^+$ and CD8$^+$ T cells are capable of expressing TLR2 (29, 59). In order to evaluate the expression of TLR2 on T cells during *B. burgdorferi* infection, flow cytometry and qRT-PCR were performed on cells from the draining lymph nodes of infected IL-10$^{-/-}$ mice. Draining lymph nodes were collected 2 weeks post-infection and CD4$^+$, CD8$^+$, and CD19$^+$ cells were isolated by flow cytometry. *Tlr2* transcripts were significantly elevated in both T and B cells following *B. burgdorferi* infection (Figure 6A). The increase of *Tlr2* transcript was specific, as *Tlr1, Tlr6, Tlr7,* and *Tlr9* transcripts remained unchanged (Figure S4A–D). At peak arthritis severity, the total number of CD4$^+$ and CD8$^+$ T cells expressing TLR2 protein had increased approximately 10-fold compared to mock-infected mice, indicating the potent ability of *B. burgdorferi* to upregulate TLR2 on T cells (Figure 6B). The expression of TLR2 on both CD4$^+$ and CD8$^+$ T cells increased and peaked at 3 weeks post-infection (Figure 6C and 6D). This finding also coincided with the highest number of CD4$^+$IFN-γ$^+$ and CD8$^+$IFN-γ$^+$ T cells in the draining lymph node (Figure 1D). In order to determine if this occurred in the absence of a *B. burgdorferi*-specific TCR, we analyzed the expression of TLR2 in both SMARTA/TCRα$^{-/-}$/IL-10$^{-/-}$ and OT-I/Rag2$^{-/-}$/IL-10$^{-/-}$ mice. TLR2 expression was increased on both CD4$^+$ and CD8$^+$ TCR transgenic T cells upon *B. burgdorferi* infection as evidenced by the increase in frequency and total

number of TLR2$^+$ T cells (Figure 6E–H). These results indicate that *B. burgdorferi* infection leads to increased transcription and expression of TLR2 on both CD4$^+$ and CD8$^+$ T cells, and could play a role in T cell activation.

TLR2 expression on T cells enhances IFN-γ production and Lyme arthritis

The observation of *B. burgdorferi*-induced TLR2 expression on T cells prompted us to directly assess its role in arthritis development. C57BL/6 Rag1$^{-/-}$ mice were infected with *B. burgdorferi* two weeks prior to an intravenous injection of T cells isolated from the lymph nodes and spleens of healthy naïve WT or TLR2$^{-/-}$ C57BL/6 mice in a method described previously (19). In this experiment donor and recipient mice expressed IL-10. Infected Rag1$^{-/-}$ mice that did not receive T cells served as controls and had mild arthritis at 5 weeks post infection (Figure 7A and 7B). Rag1$^{-/-}$ mice reconstituted with WT T cells developed severe arthritis compared to controls. Strikingly, mice which had received TLR2$^{-/-}$ T cells were protected from severe arthritis as measured by ankle swelling and histopathology scores (Figure 7B and 7C). Mice which had received WT T cells had a significant increase in serum IFN-γ compared to mice receiving TLR2$^{-/-}$ T cells. There was no IFN-γ in the serum of mice that were not reconstituted with T cells (Figure 7D). Furthermore, mice which had received WT T cells displayed an increase in *Ifng, Cxcl9*, and *Cxcl10* transcripts in the joint compared to mice reconstituted with TLR2$^{-/-}$ T cells (Figure 7E–G). IFN-γ was still present in the serum and joints of mice receiving TLR2$^{-/-}$ T cells indicating that other receptors for microbial patterns could contribute to the IFN-γ profile and the development of arthritis. It is also possible that other cytokines could also be contributing to bystander activation of T cells. Interestingly, the presence of either WT or TLR2$^{-/-}$ T cells drastically reduced the bacterial burden in the joint (Figure 7F), suggesting T cells play a role in enhancing host defense independent of TLR2. Together these data reveal TLR2 as a critical mediator of T cell activation following *B. burgdorferi* infection, which results in enhanced IFN-γ production and Lyme arthritis.

Discussion

We conclude that persistent Lyme arthritis can be initiated and sustained through bystander activation of both CD4$^+$ and CD8$^+$ T cells. This is consistent with the absence of selective expansion of any individual Vβ subset on either CD4$^+$ or CD8$^+$ T cells during *B. burgdorferi* infection. Furthermore, antigen-independent expansion and activation of TCR transgenic CD4$^+$ or CD8$^+$ T cells was sufficient to induce arthritis. *B. burgdorferi* sequentially express an abundance of lipoproteins which are critical in the activation of TLR2 expressed by innate immune cells. We now demonstrate *B. burgdorferi* induces TLR2 expression on T cells, which results in increased T cell activation and arthritis development. To our knowledge, this is the first example of CD4$^+$ T cells or CD8$^+$ T cells promoting arthritis pathogenesis in an TCR-independent mechanism.

Dysregulated immune responses are thought to play a key role in the pathogenesis of arthritis development. For example, Lyme disease patients with persisting symptoms after completing the standard dose of antibiotics often have lower frequencies of T regulatory (Treg) cells and higher expression of co-activation receptors in their synovial fluid (31). This

suggests that an inappropriately amplified immune response is contributing to arthritis development Other studies have shown that chronic states of inflammation involving both systemic and local production of pro-inflammatory cytokines such as TNF and IL-6 are required for the pathogenesis of rheumatoid arthritis (60, 61). These results suggest future CD4$^+$ and CD8$^+$ T cell studies should focus on co-stimulatory signals known to influence T cell activation and their role in Lyme and other arthralgias.

The involvement of T cells in Lyme arthritis development and resolution has been debated. Several reports suggest the adaptive immune response is not required for acute Lyme arthritis development in genetically susceptible mouse strains (C3H), as *scid* and *rag* mice, which lack both functional B and T cells, develop arthritis upon *B. burgdorferi* infection (52, 62). However, adoptive transfer of CD4$^+$ T cells into *rag* mice was shown to exacerbate the severity of Lyme arthritis, implicating a role for dysregulated T cells in Lyme disease (19). Efforts have been made to understand the protective and disease-promoting roles of the antigen-specific T cell response to *B. burgdorferi* (19, 34, 55). Initial studies suggested that T cell responses to a spirochetal epitope were cross-reacting with a similar epitope of a self-protein, resulting in molecular mimicry and autoimmune-like pathology (63). In support of this autoimmunity hypothesis, specific HLA-DR alleles such as DRB1*0101 and DRB1*01 have been linked as genetic risk factors for the development of antibiotic refractory arthritis (64). Recent studies have also identified autoantigens are capable of acting as T cell targets in patients with Lyme disease (13, 65–67). Bystander activation of T cells may provide an environment for autoimmune-mediated disease development. Previous studies have identified bystander activation of γδ T cells in synovial fluid of patients with persistent symptoms, which is dependent on TLR-activation of myeloid cells (36, 37). The mechanism by which these T cells are activated has yet to be determined, and future studies are needed to identify the primary signals which promote bystander activation. Our studies clearly provide a potential scenario in which localized activation of bystander T cells could results in the expansion of clones recognizing self-antigens.

Antigen-independent or bystander T cell activation was first demonstrated in virally-infected mice, which resulted in expansion and proliferation of heterologous polyclonal T cells (68). More recent studies have begun to illuminate the mechanisms driving this TCR-independent expansion of T cells and have implicated certain pro-inflammatory cytokines such as IFN-γ, IL-12, IL-15, and IL-18 as capable of causing bystander activation of mucosal associated variant T (MAIT) cells and memory CD8$^+$ T cells (69–73). However, less is known about the signals which initiate CD4$^+$ T cell bystander activation. The ability of both CD4$^+$ and CD8$^+$ T cell bystander activation to exacerbate Lyme arthritis is unique. The presence of CD8$^+$ T cells was sufficient to fully promote Lyme arthritis in IL-10$^{-/-}$ mice, despite the absence of CD4$^+$ T cells and B cells. CD4$^+$ T cells have a dual role in host pathogenesis and host defense in this model system, as bacterial burden in the joints was higher in the absence of CD4$^+$ T cells. Differences in bacterial load between IL-10$^{-/-}$ and CD4 TCR transgenic mice indicate that while a *Borrelia*-specific CD4$^+$ T cell response is required for clearance of *B. burgdorferi*, it is not required to promote arthritis severity. This finding is consistent with previous publications using other mouse strains which show that *Borrelia* load does not correlate with arthritis severity (74, 75). It was also revealed that CD4$^+$ T cells play a role in the generation of *B. burgdorferi*-specific antibodies, as their absence during infection

resulted in decreased *B. burgdorferi*-specific IgG. This unique host defense feature of CD4^{+} T cells is not shared by CD8^{+} T cells, and implicates a role for CD4^{+} T cell antigen specificity in promoting bacterial clearance. Our findings suggest that CD8^{+} T cells could even provide a therapeutic target for control of inflammation without compromising the ability to clear infection.

Several studies have reported a co-stimulatory role for TLRs on CD8^{+} T cells. TLR2 expression on CD8^{+} T cells leads to a decreased activation threshold for co-stimulatory signals received by antigen-presenting cells (APCs) (76). Our data supports these results as TLR2 expression increased on both CD4^{+} and CD8^{+} T cells during *B. burgdorferi* infection. The expression of TLR2 on T cells also coincided with the increase in IFN-γ^+ T cells, further suggesting that TLR2 is playing a direct role in IFN-γ secretion. Strikingly, arthritis severity was greatly reduced when TLR2 was selectively missing from T cells, revealing TLR2 as a critical component of bystander T cell activation driving arthritis. Accumulating evidence supports significant alterations in T cell TLR expression in patients with infectious diseases. For example, T cells from patients with chronic hepatitis C express higher transcript levels of several TLRs in CD8^{+} T cells compared to healthy controls (77). More studies are needed to assess the effect of altered TLR expression on T cells and its contribution to pathogenesis and immune defense.

This study highlights the antigen-independent role of both CD4^{+} and CD8^{+} T cells in the development of Lyme arthritis. Importantly, several observations in the IL-10^{−/−} mouse model are recapitulated in post-treatment Lyme disease patients (31, 32). Synovial tissue from patients contains elevated numbers of CD4^{+} T cells, as well as elevated concentrations of IFN-γ, CXCL9 and CXCL10 compared to patients whose arthritis resolves after antibiotics. This is unique, as other mouse models have not allowed for the assessment of T cell contribution. Therefore, our study reveals a role for T cell driven arthritis, providing insight into the pathogenic potential of inflammatory dysregulation in Lyme disease.

Supplementary Material

Refer to Web version on PubMed Central for supplementary material.

Acknowledgments

References

1. Hu LT. In the clinic®: Lyme disease. Ann. Intern. Med. 2016; 164:ITC65–ITC79. [PubMed: 27136224]

2. Steere AC, Schoen RT, Taylor E. The clinical evolution of lyme arthritis. Ann. Intern. Med. 1987; 107:725–731. [PubMed: 3662285]

3. Cimmino MA, Moggiana GL, Parisi M, Accardo S. Treatment of Lyme arthritis. Infection. 1996; 24:91–94. [PubMed: 8852480]

4. Steere AC, Angelis SM. Therapy for lyme arthritis: Strategies for the treatment of antibiotic-refractory arthritis. Arthritis Rheum. 2006; 54:3079–3086. [PubMed: 17009226]

5. Wills AB, Spaulding AB, Adjemian J, Prevots DR, Turk SP, Williams C, Marques A. Long-term Follow-up of Patients with Lyme Disease: Longitudinal Analysis of Clinical and Quality-of-life Measures. Clin. Infect. Dis. 2016; 62:1546–1551. [PubMed: 27025825]

6. Nocton JJ, Dressler F, Rutledge BJ, Rys PN, Persing DH, Steere AC. Detection of Borrelia burgdorferi DNA by polymerase chain reaction in synovial fluid from patients with Lyme arthritis. N Engl. J. Med. 1994; 330:229–234. [PubMed: 8272083]

7. Li X, McHugh GA, Damle N, Sikand VK, Glickstein L, Steere AC. Burden and viability of Borrelia burgdorferi in skin and joints of patients with erythema migrans or lyme arthritis. Arthritis Rheum. 2011; 63:2238–2247. [PubMed: 21590753]

8. Radolf J. Posttreatment chronic Lyme disease--what it is not. J Infect. Dis. 2005; 192:948–9. [PubMed: 16107945]

9. Shen S, Shin JJ, Strle K, McHugh G, Li X, Glickstein LJ, Drouin EE, Steere AC. Treg cell numbers and function in patients with antibiotic-refractory or antibiotic-responsive lyme arthritis. Arthritis Rheum. 2010; 62:2127–2137. [PubMed: 20506317]

10. Gross DM, Steere AC, Huber BT. T helper 1 response is dominant and localized to the synovial fluid in patients with Lyme arthritis. J Immunol. 1998; 160:1022–1028. [PubMed: 9551943]

11. Yudoh K, Matsuno H, Nakazawa F, Yonezawa T, Kimura T. Reduced expression of the regulatory CD4+ T cell subset is related to Th1/Th2 balance and disease severity in rheumatoid arthritis. Arthritis Rheum. 2000; 43:617–627. [PubMed: 10728756]

12. Steere AC, Dwyer E, Winchester R. Association of chronic Lyme arthritis with HLA-DR4 and HLA-DR2 alleles. N Engl. J. Med. 1990; 323:219–230. [PubMed: 2078208]

13. Pianta A, Drouin EE, Crowley JT, Arvikar S, Strle K, Costello CE, Steere AC. Annexin A2 is a target of autoimmune T and B cell responses associated with synovial fibroblast proliferation in patients with antibiotic-refractory Lyme arthritis. Clin. Immunol. 2015; 160:336–341. [PubMed: 26187145]

14. Steere AC, Glickstein L. Elucidation of Lyme arthritis. Nat. Rev. Immunol. 2004; 4:143–52. [PubMed: 15040587]

15. Girschick HJ, Huppertz HI, Rüssmann H, Krenn V, Karch H. Intracellular persistence of Borrelia burgdorferi in human synovial cells. Rheumatol. Int. 1996; 16:125–32. [PubMed: 8893378]

16. Bockenstedt LK, Gonzalez DG, Haberman AM, Belperron AA. Spirochete antigens persist near cartilage after murine Lyme borreliosis therapy. J Clin. Invest. 2012; 122:2652–2660. [PubMed: 22728937]

17. Embers ME, Barthold SW, Borda JT, Bowers L, Doyle L, Hodzic E, Jacobs MB, Hasenkampf NR, Martin DS, Narasimhan S, Phillippi-Falkenstein KM, Purcell JE, Ratterree MS, Philipp MT. Persistence of borrelia burgdorferi in rhesus macaques following antibiotic treatment of disseminated infection. PLoS One. 2012; 7:e29914. [PubMed: 22253822]

18. Geissmann F, Cameron TO, Sidobre S, Manlongat N, Kronenberg M, Briskin MJ, Dustin ML, Littman DR. Intravascular immune surveillance by CXCR6+ NKT cells patrolling liver sinusoids. PLoS Biol. 2005; 3:0650–0661.

19. McKisic MD, Redmond WL, Barthold SW. Cutting edge: T cell-mediated pathology in murine Lyme borreliosis. J Immunol. 2000; 164:6096–9. [PubMed: 10843657]

20. Fraser C, Casjens S, Huang W. Genomic sequence of a Lyme disease spirochaete, Borrelia burgdorferi. Nature. 1997; 390:580–586. [PubMed: 9403685]

21. Hirschfeld M, Kirschning CJ, Schwandner R, Wesche H, Weis JH, Wooten RM, Weis JJ. Inflammatory Signaling by Borrelia burgdorferi Lipoproteins Is Mediated by Toll-Like Receptor 2. J Immunol. 1999; 163:2382–2386. [PubMed: 10452971]

22. Alexopoulou L, Thomas V, Schnare M, Lobet Y, Anguita J, Schoen RT, Medzhitov R, Fikrig E, Flavell Ra. Hyporesponsiveness to vaccination with Borrelia burgdorferi OspA in humans and in TLR1- and TLR2-deficient mice. Nat. Med. 2002; 8:878–84. [PubMed: 12091878]

23. Radolf JD, Caimano MJ, Stevenson B, Hu LT. Of ticks, mice and men: understanding the dual-host lifestyle of Lyme disease spirochaetes. Nat. Rev. Microbiol. 2012; 10:87–99. [PubMed: 22230951]

24. Fikrig E, Barthold SW, Kantor FS, Flavell RA. Protection of mice against the Lyme disease agent by immunizing with recombinant OspA. Science. 1990; 250:553–556. [PubMed: 2237407]

25. Wooten RM, Ma Y, Yoder RA, Brown JP, Weis JH, Zachary JF, Kirschning CJ, Weis JJ. Toll-like receptor 2 is required for innate, but not acquired, host defense to Borrelia burgdorferi. J Immunol. 2002; 168:348–55. [PubMed: 11751980]

26. Wang X, Ma Y, Yoder A, Crandall H, Zachary JF, Fujinami RS, Weis JH, Weis JJ. T cell infiltration is associated with increased Lyme arthritis in TLR2–/– mice. FEMS Immunol. Med. Microbiol. 2008; 52:124–33. [PubMed: 18081848]

27. Lasky CE, Pratt CL, Hilliard KA, Jones JL, Brown CR. T cells exacerbate lyme borreliosis in TLR2-deficient mice. Front. Immunol. 2016; 7:468. [PubMed: 27857714]

28. Komai-Koma M, Jones L, Ogg GS, Xu D, Liew FY. TLR2 is expressed on activated T cells as a costimulatory receptor. Proc. Natl. Acad. Sci. U. S. A. 2004; 101:3029–34. [PubMed: 14981245]

29. Round JL, Lee SM, Li J, Tran G, Jabri B, Chatila TA, Mazmanian SK. The Toll-like receptor pathway establishes commensal gut colonization. Science. 2011; 332:974–977. [PubMed: 21512004]

30. Abdollahi-Roodsaz SL, Joosten AB, Koenders MI, Devesa I, Roelofs MF, Radstake TRDJ, Heuvelmans-Jacobs M, Akira S, Nicklin MJH, Ribeiro-Dias F, Van Den Berg WB. Stimulation of TLR2 and TLR4 differentially skews the balance of T cells in a mouse model of arthritis. J Clin. Invest. 2008; 118:205–216. [PubMed: 18060042]

31. Vudattu NK, Strle K, Steere AC, Drouin EE. Dysregulation of CD4+CD25high T cells in the synovial fluid of patients with antibiotic-refractory lyme arthritis. Arthritis Rheum. 2013; 65:1643–1653. [PubMed: 23450683]

32. Soloski MJ, Crowder LA, Lahey LJ, Wagner CA, Robinson WH, Aucott JN. Serum inflammatory mediators as markers of human lyme disease activity. PLoS One. 2014; 9:e93243. [PubMed: 24740099]

33. Shen S, Shin JJ, Strle K, McHugh G, Li X, Glickstein LJ, Drouin EE, Steere AC. Treg cell numbers and function in patients with antibiotic-refractory or antibiotic-responsive lyme arthritis. Arthritis Rheum. 2010; 62:2127–2137. [PubMed: 20506317]

34. Kang I, Barthold SW, Persing DH, Bockenstedt LK, Kang I, Barthold SW, Persing DH. T-helper-cell cytokines in the early evolution of murine Lyme arthritis. Infect. Immun. 1997; 65:3107–3111. [PubMed: 9234761]

35. Matyniak JE, Reiner SL. T helper phenotype and genetic susceptibility in experimental Lyme disease. J Emerg. Med. 1995; 181:1251–4.

36. Collins C, Shi C, Russell JQ, Fortner Ka, Budd RC. Activation of gamma delta T cells by Borrelia burgdorferi is indirect via a TLR- and caspase-dependent pathway. J Immunol. 2008; 181:2392–8. [PubMed: 18684928]

37. Vincent MS, Roessner K, Lynch D, Wilson D, Cooper SM, Tschopp J, Sigal LH, Budd RC. Apoptosis of Fashigh CD4+ synovial T cells by borrelia-reactive Fas-ligand(high) gamma delta T cells in Lyme arthritis. J Exp. Med. 1996; 184:2109–17. [PubMed: 8976167]

38. Vincent MS, Roessner K, Sellati T, Huston CD, Sigal LH, Behar SM, Radolf JD, Budd RC. Lyme arthritis synovial gamma delta T cells respond to Borrelia burgdorferi lipoproteins and lipidated hexapeptides. J Immunol. 1998; 161:5762–5771. [PubMed: 9820558]

39. Sonderegger FL, Ma Y, Maylor-Hagan H, Brewster J, Huang X, Spangrude GJ, Zachary JF, Weis JH, Weis JJ. Localized production of IL-10 suppresses early inflammatory cell infiltration and subsequent development of IFN-γ-mediated Lyme arthritis. J Immunol. 2012; 188:1381–93. [PubMed: 22180617]

40. Lochhead RB, Zachary JF, Rosa LD, Ma Y, Weis JH, O'Connell RM, Weis JJ. Antagonistic Interplay between MicroRNA-155 and IL-10 during Lyme Carditis and Arthritis. PLoS One. 2015; 10:e0135142. [PubMed: 26252010]

41. Aletaha D, Tsonaka R, Gaujoux-Viala C, Fautrel B, van der A, Mil H, Zinkernagel R, Steere AC. Two rheumatoid arthritis–specific autoantigens correlate microbial immunity with autoimmune responses in joints. Arthritis Rheum. 2017; 62:2569–2581.

42. Oxenius, a, Bachmann, MF., Zinkernagel, RM., Hengartner, H. Virus-specific MHC-class II-restricted TCR-transgenic mice: effects on humoral and cellular immune responses after viral infection. Eur. J. Immunol. 1998; 28:390–400. [PubMed: 9485218]

43. Liu F, Whitton JL. Cutting Edge: Re-evaluating the In Vivo Cytokine Responses of CD8+ T Cells during Primary and Secondary Viral Infections. J Immunol. 2005; 174:5936–5940. [PubMed: 15879085]

44. Lochhead RB, Ma Y, Zachary JF, Baltimore D, Zhao JL, Weis JH, O'Connell RM, Weis JJ. MicroRNA-146a Provides Feedback Regulation of Lyme Arthritis but Not Carditis during Infection with Borrelia burgdorferi. PLoS Pathog. 2014; 10:e1004212. [PubMed: 24967703]

45. Ornstein K, Barbour AG. A reverse transcriptase-polymerase chain reaction assay of Borrelia burgdorferi 16S rRNA for highly sensitive quantification of pathogen load in a vector. Vector-Borne Zoonotic Dis. 2006; 6:103–112. [PubMed: 16584333]

46. Crandall H, Dunn DM, Ma Y, Wooten RM, Zachary JF, Weis JH, Weiss RB, Weis JJ. Gene expression profiling reveals unique pathways associated with differential severity of lyme arthritis. J Immunol. 2006; 177:7930–7942. [PubMed: 17114465]

47. Miller JC, Ma Y, Bian J, Sheehan KCF, Zachary JF, Weis JH, Schreiber RD, Weis JJ. A critical role for type I IFN in arthritis development following Borrelia burgdorferi infection of mice. J Immunol. 2008; 181:8492–503. [PubMed: 19050267]

48. Brown JP, Zachary JF, Teuscher C, Weis JJ, Wooten RM. Dual role of interleukin-10 in murine lyme disease: Regulation of arthritis severity and host defense. Infect. Immun. 1999; 67:5142–5150. [PubMed: 10496888]

49. Strle K, Sulka KB, Pianta A, Crowley JT, Arvikar SL, Anselmo A, Sadreyev R, Steere AC. T-helper 17 cell cytokine responses in lyme disease correlate with borrelia burgdorferi antibodies during early infection and with autoantibodies late in the illness in patients with antibiotic-refractory lyme arthritis. Clin. Infect. Dis. 2017; 64:930–938. [PubMed: 28077518]

50. Arvikar SL, Crowley JT, Sulka KB, Steere AC. Autoimmune Arthritides, Rheumatoid Arthritis, Psoriatic Arthritis, or Peripheral Spondyloarthritis Following Lyme Disease. Arthritis Rheumatol. 2017; 69:194–202. [PubMed: 27636905]

51. Brown CR, Reiner SL. Experimental lyme arthritis in the absence of interleukin-4 or gamma interferon. Infect. Immun. 1999; 67:3329–3333. [PubMed: 10377109]

52. Barthold SW, Sidman CL, Smith AL. Lyme borreliosis in genetically resistant and susceptible mice with severe combined immunodeficiency. Am. J. Trop. Med. Hyg. 1992; 47:605–613. [PubMed: 1449201]

53. Shin JJ, Glickstein LJ, Steere AC. High levels of inflammatory chemokines and cytokines in joint fluid and synovial tissue throughout the course of antibiotic-refractory lyme arthritis. Arthritis Rheum. 2007; 56:1325–1335. [PubMed: 17393419]

54. Glickstein L, Edelstein M, Dong JZ. Gamma interferon is not required for arthritis resistance in the murine Lyme disease model. Infect. Immun. 2001; 69:3737–3743. [PubMed: 11349038]

55. Elsner RA, Hastey CJ, Baumgarth N. CD4+ T cells promote antibody production but not sustained affinity maturation during Borrelia burgdorferi infection. Infect. Immun. 2015; 83:48–56. [PubMed: 25312948]

56. Williams MA, Ravkov EV, Bevan MJ. Rapid Culling of the CD4+ T Cell Repertoire in the Transition from Effector to Memory. Immunity. 2008; 28:533–545. [PubMed: 18356084]

57. Kim C, Wilson T, Fischer KF, Williams MA. Sustained interactions between T cell receptors and antigens promote the differentiation of CD4+ memory T cells. Immunity. 2013; 39:508–520. [PubMed: 24054329]

58. Horrocks C, Holder JE, Berth-Jones J, Camp RD. Antigen-independent expansion of T cells from psoriatic skin lesions: phenotypic characterization and antigen reactivity. Br. J. Dermatol. 1997; 137:331–338. [PubMed: 9349325]

59. Reynolds JM, Pappu BP, Peng J, Martinez GJ, Zhang Y, Chung Y, Ma L, Yang XO, Nurieva RI, Tian Q, Dong C. Toll-like receptor 2 signaling in CD4+ T lymphocytes promotes T helper 17 responses and regulates the pathogenesis of autoimmune disease. Immunity. 2010; 32:692–702. [PubMed: 20434372]

60. Williams RO, Feldmann M, Maini RN. Anti-tumor necrosis factor ameliorates joint disease in murine collagen-induced arthritis. Proc. Natl. Acad. Sci. U. S. A. 1992; 89:9784–9788. [PubMed: 1409699]

61. Fujimoto M, Serada S, Mihara M, Uchiyama Y, Yoshida H, Koike N, Ohsugi Y, Nishikawa T, Ripley B, Kimura A, Kishimoto T, Naka T. Interleukin-6 blockade suppresses autoimmune arthritis in mice by the inhibition of inflammatory Th17 responses. Arthritis Rheum. 2008; 58:3710–3719. [PubMed: 19035481]

62. Brown CR, Reiner SL. Genetic control of experimental Lyme arthritis in the absence of specific immunity. Infect. Immun. 1999; 67:1967–1973. [PubMed: 10085044]

63. Gross DM, Forsthuber T, Tary-Lehmann M, Etling C, Ito K, Nagy ZA, Field JA, Steere AC, Huber BT. Identification of LFA-1 as a candidate autoantigen in treatment-resistant Lyme arthritis. Science. 1998; 281:703–706. [PubMed: 9685265]

64. Steere AC, Klitz W, Drouin EE, Falk Ba, Kwok WW, Nepom GT, Baxter-Lowe LA. Antibiotic-refractory Lyme arthritis is associated with HLA-DR molecules that bind a Borrelia burgdorferi peptide. J Exp. Med. 2006; 203:961–971. [PubMed: 16585267]

65. Drouin EE, Seward RJ, Strle K, McHugh G, Katchar K, Londono D, Yao C, Costello CE. A novel human autoantigen, endothelial cell growth factor, is a target of T and B cell responses in patients with Lyme disease. Arthritis Rheum. 2013; 65:186–196. [PubMed: 23044924]

66. Crowley JT, Drouin EE, Pianta A, Strle K, Wang Q, Costello CE, Steere AC. A Highly Expressed Human Protein, Apolipoprotein B-100, Serves as an Autoantigen in a Subgroup of Patients with Lyme Disease. J Infect. Dis. 2015; 212:1841–1850. [PubMed: 26014802]

67. Pianta A, Arvikar SL, Strle K, Drouin EE, Wang Q, Costello CE, Steere AC. Two rheumatoid arthritis-specific autoantigens correlate microbial immunity with autoimmune responses in joints. J Clin. Invest. 2017; 127:2946–2956. [PubMed: 28650341]

68. Tough DF, Borrow P, Sprent J. Induction of bystander T cell proliferation by viruses and type I interferon in vivo. Science. 1996; 272:1947–50. [PubMed: 8658169]

69. Tough DF, Zhang X, Sprent J. An IFN-gamma-dependent pathway controls stimulation of memory phenotype CD8+ T cell turnover in vivo by IL-12, IL-18, and IFN-gamma. J Immunol. 2001; 166:6007–11. [PubMed: 11342616]

70. Zhang X, Sun S, Hwang I, Tough DF, Sprent J. Potent and selective stimulation of memory-phenotype CD8+ T cells in vivo by IL-15. Immunity. 1998; 8:591–599. [PubMed: 9620680]

71. Slichter CK, McDavid A, Miller HW, Finak G, Seymour BJ, McNevin JP, Diaz G, Czartoski JL, McElrath MJ, Gottardo R, Prlic M. Distinct activation thresholds of human conventional and innate-like memory T cells. JCI insight. 2016; 1:193–201.

72. McSorley SJ. The role of non-cognate T cell stimulation during intracellular bacterial infection. Front. Immunol. 2014; 5:319. [PubMed: 25071779]

73. O'Donnell H, McSorley SJ. Salmonella as a model for non-cognate Th1 cell stimulation. Front. Immunol. 2014; 5:621. [PubMed: 25540644]

74. Brown CR, Reiner SL. Clearance of Borrelia burgdorferi may not be required for resistance to experimental Lyme arthritis. Infect. Immun. 1998; 66:2065–2071. [PubMed: 9573090]

75. Ma Y, Seiler KP, Eichwald EJ, Weis JH, Teuscher C, Weis JJ. Distinct characteristics of resistance to Borrelia burgdorferi induced arthritis in C57BL/6N mice. Infect. Immun. 1998; 66:161–168. [PubMed: 9423853]

76. Cottalorda A, Verschelde C, Marçais A, Tomkowiak M, Musette P, Uematsu S, Akira S, Marvel J, Bonnefoy-Berard N. TLR2 engagement on CD8 T cells lowers the threshold for optimal antigen-induced T cell activation. Eur. J. Immunol. 2006; 36:1684–1693. [PubMed: 16761317]
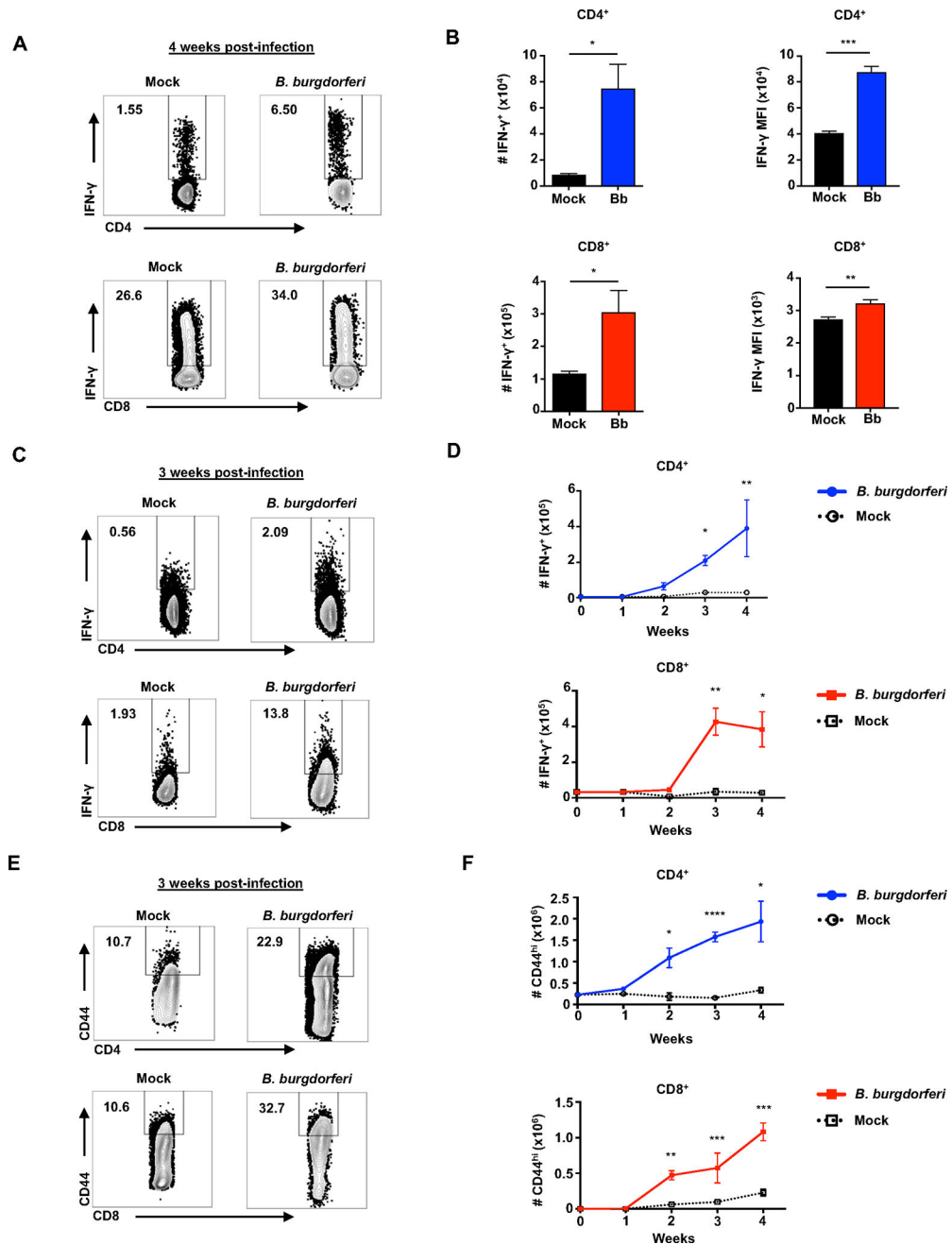
77. Dolganiuc A, Garcia C, Kodys K, Szabo G. Distinct Toll-like receptor expression in monocytes and T cells in chronic HCV infection. World J. Gastroenterol. 2006; 12:1198–1204. [PubMed: 16534871]

Figure 1. CD4⁺ and CD8⁺ T cells produce IFN-γ throughout *B. burgdorferi* infection
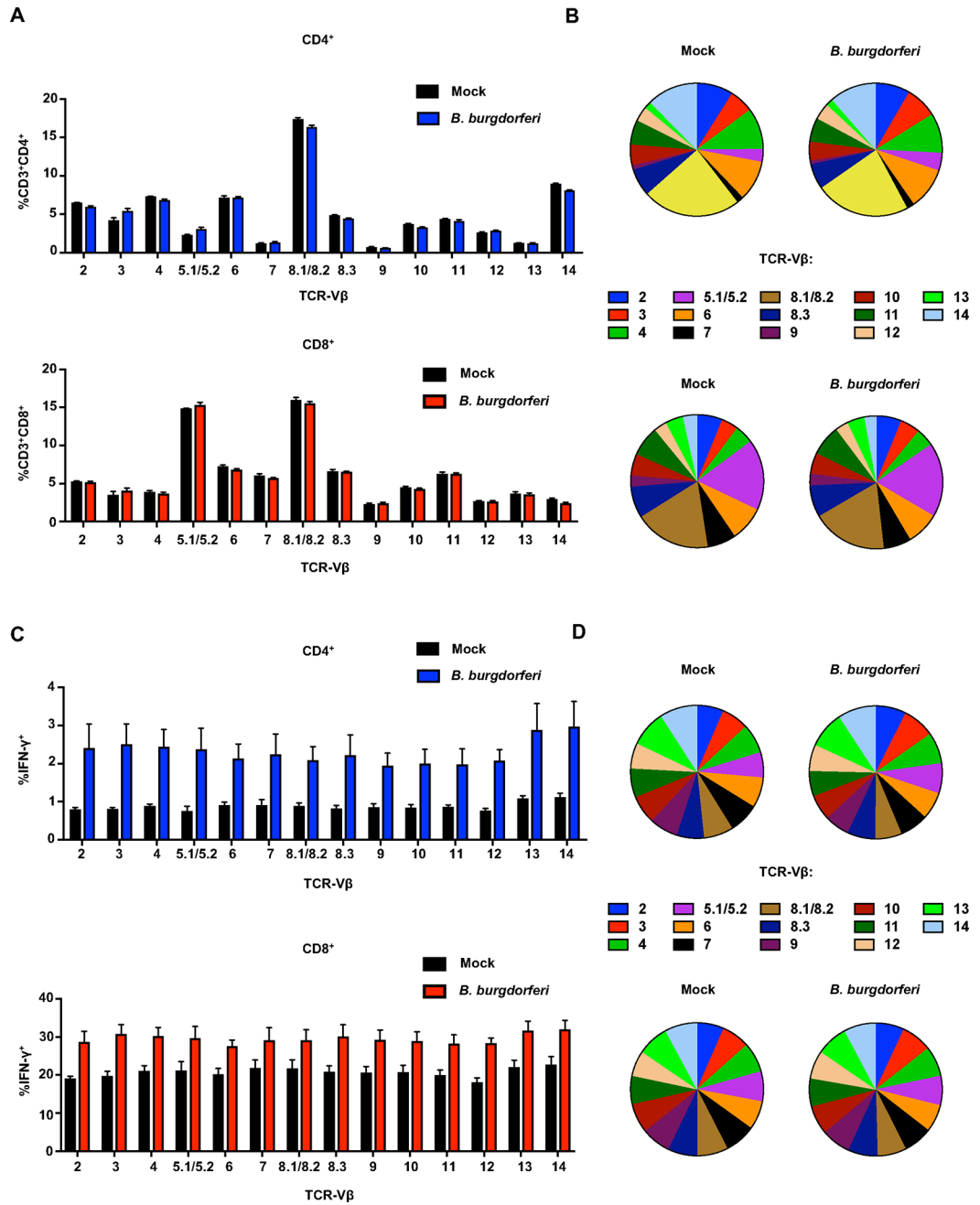
IL-10$^{-/-}$ mice were infected with *B. burgdorferi*, after which popliteal and inguinal lymph nodes were collected for analysis of T cells and IFN-γ production. (A) *B. burgdorferi* infected or mock-infected IL-10$^{-/-}$ mice were sacrificed after 4 weeks of infection. Representative flow plots of IFN-γ production by CD4⁺ and CD8⁺ T cells in after 4 hours of stimulation with PMA/Ionomycin in presence of Brefeldin A. Numbers in upper left corner of boxes are %IFN-γ⁺ cells. (B) The total number of IFN-γ⁺CD4⁺ and IFN-γ⁺CD8⁺ T by flow cytometry and the mean fluorescence intensity (MFI) of IFN-γ. (C–F) *B. burgdorferi* infected or mock-infected IL-10$^{-/-}$ mice were injected with Brefeldin A 6 hours before

sacrifice at 1 week time intervals for 4 weeks. (C) Representative flow plots of IFN-γ production by CD4$^+$ and CD8$^+$ T cells in *B. burgdorferi* infected or mock-infected IL-10$^{-/-}$ mice at 3 weeks of infection. Numbers in upper left corner of boxes are %IFN-γ^+ cells. (D) Total number of CD4$^+$IFN-γ^+ and CD8$^+$IFN-γ^+ T cells from infected and mock-infected IL-10$^{-/-}$ mice. (E) Representative flow plots of CD4$^+$CD44^{hi} and CD8$^+$CD44^{hi} T cells in *B. burgdorferi* infected or mock-infected IL-10$^{-/-}$ mice. Numbers in upper left corner of boxes are %CD44^{hi} cells. (F) Total number of CD4$^+$CD44^{hi} and CD8$^+$CD44^{hi} T cells from infected and mock-infected IL-10$^{-/-}$ mice. Error bars indicate the SEM (n 3 per group). Statistically significant differences between groups by Student's t-test are indicated (*p<0.05, **p<0.01, ***p<0.001 ****p<0.0001). Data are representative of two independent experiments.
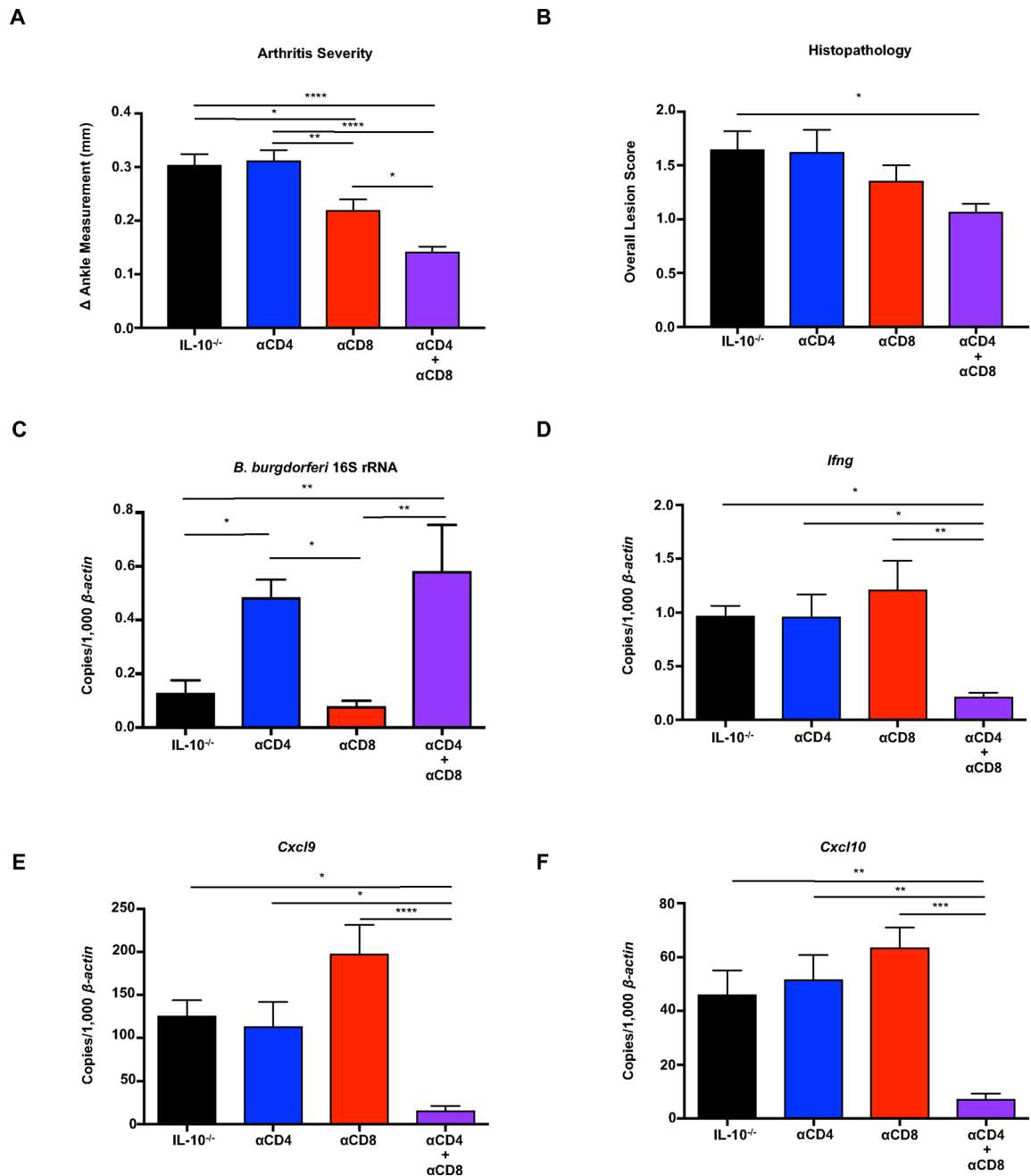
Figure 2. Both CD4^{+} and CD8^{+} T cells contribute to the development of Lyme arthritis

IL-10^{−/−} mice were infected with *B. burgdorferi* for 4 weeks, and treated with isotype control antibody, anti-CD4, anti-CD8, or both anti-CD4 and anti-CD8 throughout the infection (**Methods**). (A) Rear ankle measurements were taken before infection and 4 weeks post-infection, and the change in ankle measurement is shown. (B) The most swollen ankle was assessed by histopathologic evaluation. Scores 0–5, with 5 being most severe, were assigned to each sample. (C–F) Quantification of *B. burgdorferi*-specific *16S rRNA*, *Ifng*, *Cxcl9*, and *Cxcl10* was normalized to 1,000 *β-actin* in the joint using qRT-PCR. Error bars indicate the SEM (n ≥ 7 per group). Statistically significant differences between groups by

ANOVA followed by Bonferroni's post-hoc test are indicated (*$p<0.05$, **$p<0.01$, ***$p<0.001$ ****$p<0.0001$) (A, C–F). (B) For lesion scoring, Mann-Whitney *U* test was used to determine whether there was statistically significant difference with groups, with p values indicated.

Figure 3. *B. burgdorferi* infection results in universal expansion and activation of CD4^{+} and CD8^{+} T cells

IL-10^{−/−} mice were infected with *B. burgdorferi* for 4 weeks, after which popliteal and inguinal lymph nodes were collected for analysis of TCR repertoires. (A) and (B) Frequency of TCR Vβ-specific cells was quantified for CD3^{+}CD4^{+} (upper panel) or CD3^{+}CD8^{+} (lower panel) gated populations. (C) and (D) Frequency of TCR Vβ-specific cells was quantified for CD4^{+}IFN-γ^{+} (upper panel) and CD8^{+}IFN-γ^{+} (lower panel) gated populations. Error bars indicate the SEM (n 3 per group). Data are representative of two independent experiments.
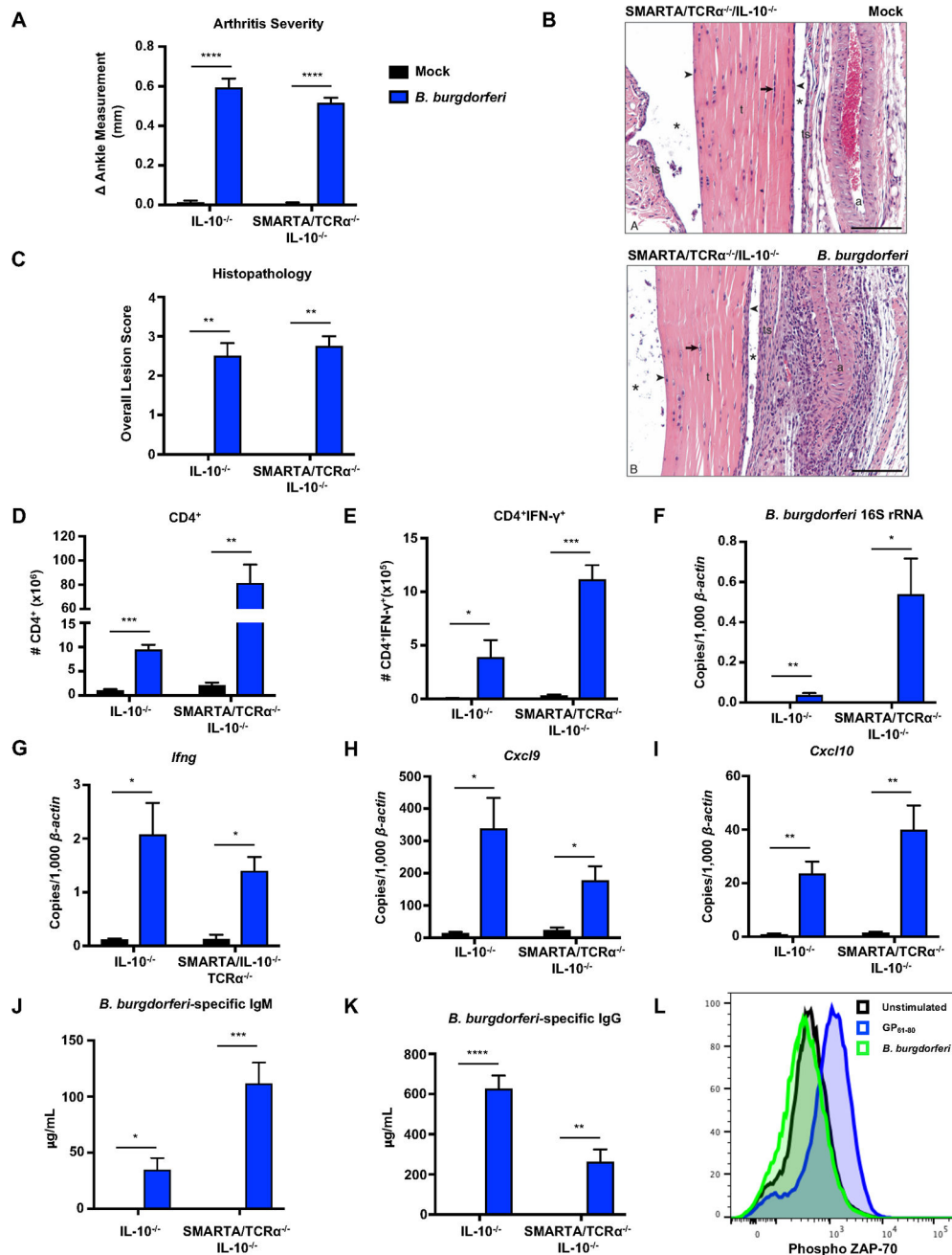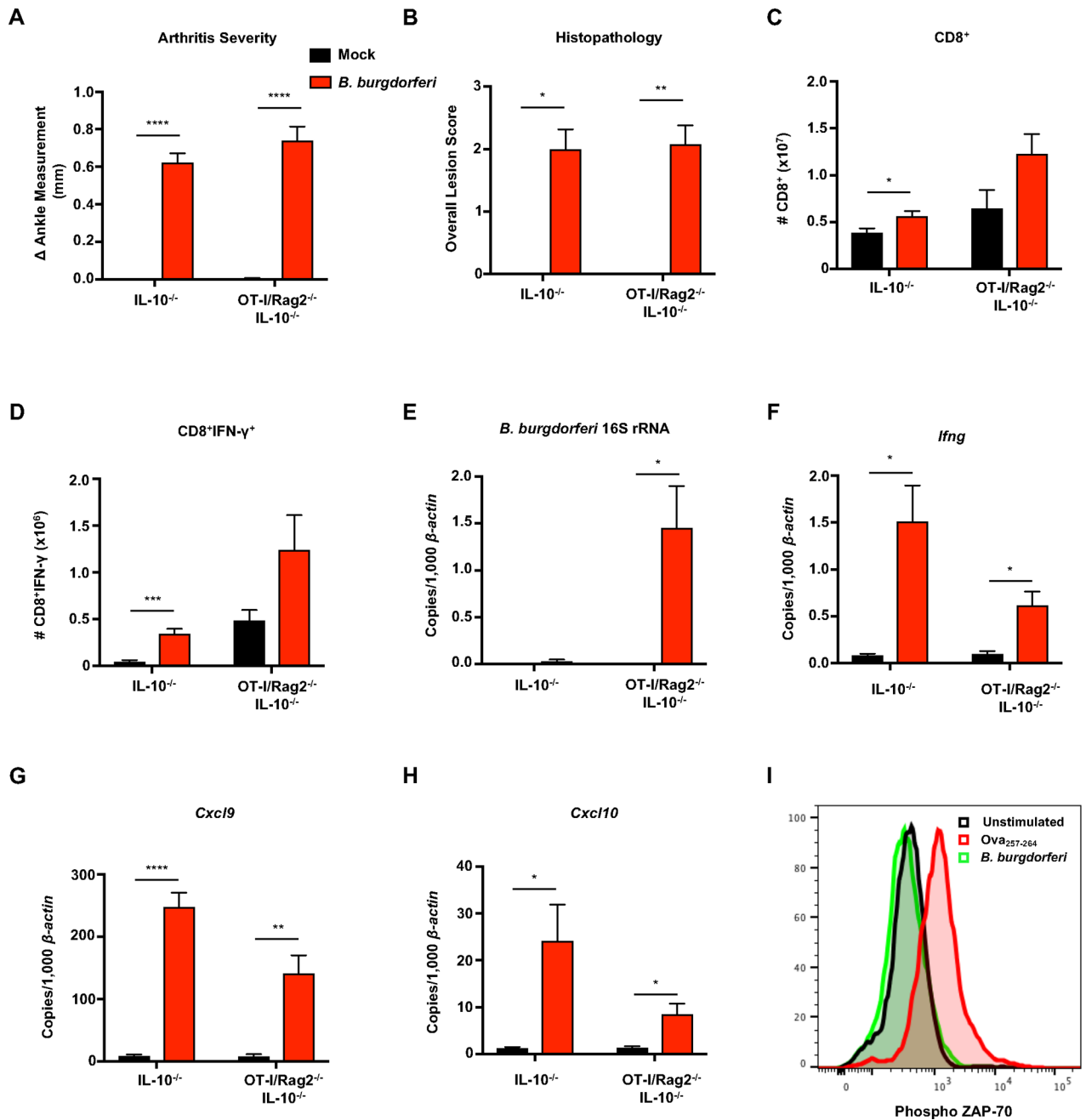
Figure 4. *B. burgdorferi* infection results in antigen-independent expansion and activation of TCR transgenic CD4+ T cells

IL-10$^{-/-}$ and CD4+ TCR transgenic SMARTA/TCRα$^{-/-}$/IL-10$^{-/-}$ mice were infected with *B. burgdorferi* for 4 weeks. (A) Measurements of rear ankles of mice were taken before infection and 4 weeks post-infection, and change in ankle measurement is shown. (B) Representative images of H&E-stained tibiotarsal joints from mock-infected (control) and 4 week-infected SMARTA/TCRα$^{-/-}$/IL-10$^{-/-}$ mice used for histopathology scoring t= tendon, * = tendon space, ts= tendon sheath, arrow = tenocytes, arrowhead = synoviocytes, a = arteriole. scale bar = 100 μm. (C) The most swollen ankle was subjected to blinded histopathologic evaluation in a blind fashion. Scores 0–5, with 5 being most severe, were

assigned to each sample. (D) The total number of CD4$^+$ T cells were quantified from the popliteal and inguinal lymph nodes. (E) Lymph node cells were stimulated with PMA/Ionomycin in presence of Brefeldin A, and the number of CD4$^+$IFN-γ^+ T cells were quantified using flow cytometry. (F–I) Quantification of *B. burgdorferi*-specific *16S rRNA*, *Ifng*, *Cxcl9*, and *Cxcl10* was normalized to 1,000 β-*actin* in the joint using qRT-PCR. (J–K) Serum was obtained from mice two weeks post-infection and assessed for *B. burgdorferi*-specific IgM (J) and *B. burgdorferi*-specific IgG (K) using sonicated *B. burgdorferi* bound to ELISA plates (**Methods**). (L) Unfractionated naive SMARTA/TCR$\alpha^{-/-}$/IL-10$^{-/-}$ splenocytes were isolated and stimulated in the presence of *B. burgdorferi* (10μg/mL) or GP$_{61–80}$ (1μM) for 3 hours. SMARTA CD4$^+$ T cells were analyzed by flow cytometry for phosphorylated ZAP-70. Error bars indicate the SEM (n 8 per group) Significant differences between mock and *B. burgdorferi* infected groups for each genotype were determined by Student's t-test, with Mann-Whitney *U* test used for categorically accessed lesion scores (C) (*p<0.05, **p<0.01, ***p<0.001 ****p<0.0001). Data are representative of two independent experiments.

Figure 5. _B. burgdorferi_ infection of CD8$^+$ TCR transgenic mice results in arthritis and IFN-γ production

IL-10$^{-/-}$ and CD8$^+$ TCR transgenic OT-I/Rag2$^{-/-}$/IL-10$^{-/-}$ mice were infected with _B. burgdorferi_ for 4 weeks. (A) Rear ankles of mice were measured before infection and 4 weeks post-infection, and change in ankle measurement is shown. (B) The most swollen ankle was subjected to histopathologic evaluation in a blind fashion. Scores 0–5, with 5 being most severe, were assigned to each sample. (C) The total number of CD8$^+$ were quantified from the popliteal and inguinal lymph nodes. (D) Lymph node cells were stimulated with PMA/Ionomycin in presence of Brefeldin A, and the number of CD8$^+$IFN-γ$^+$ T cells were quantified using flow cytometry. (E–I) Quantification of _B. burgdorferi-_

specific *16S rRNA*, *Ifng*, *Cxcl9*, and *Cxcl10* was normalized to 1,000 *β-actin* in the joint using qRT-PCR. (J) Unfractionated naive OT-I/Rag2$^{-/-}$/IL-10$^{-/-}$ splenocytes were isolated and stimulated in the presence of *B. burgdorferi* (10μg/mL) or Ova$_{257-264}$ (1μM) for 3 hours. OT-I CD8$^+$ T cells were analyzed by flow cytometry for phosphorylated ZAP-70. Error bars indicate the SEM (n 5 per group). Significant differences between infected and uninfected groups for each genotype are indicated by Student's t-test (*p<0.05, **p<0.01). For lesion scoring, Mann-Whitney *U* test was used to determine statistically significant differences with groups, with p values indicated. Data are representative of two independent experiments.
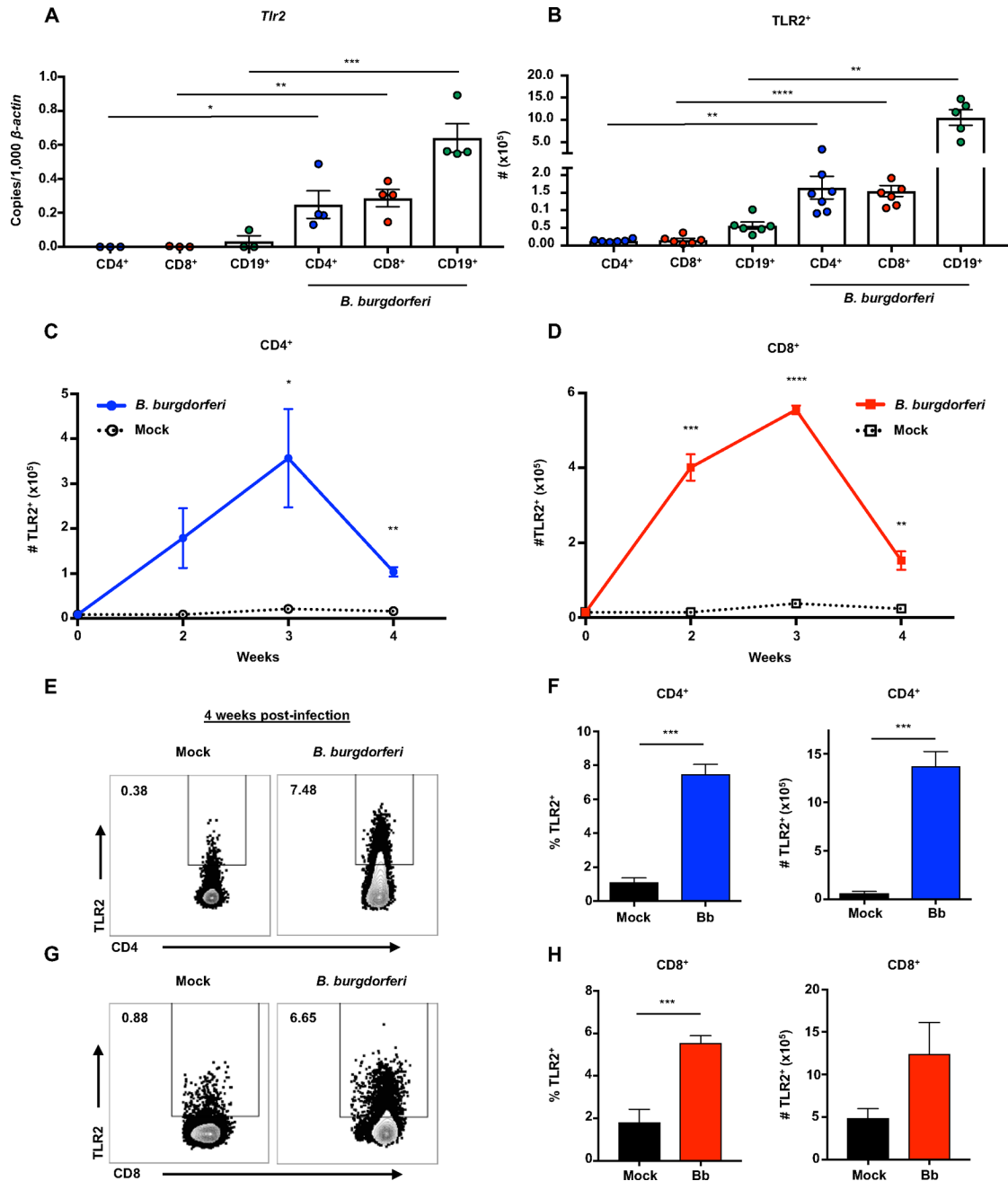
Figure 6. T cells display increased transcription and expression of TLR2 following *B. burgdorferi* infection

Mice were infected with *B. burgdorferi*, after which popliteal and inguinal lymph nodes were collected for analysis of T cells and TLR2 expression. (A) CD3+CD4+, CD3+CD8+, and CD19+ cells were sorted from popliteal and inguinal lymph nodes of IL-10−/− mice using FACS sorting (BD FACSAria) 2 weeks post-infection. *Tlr2* transcripts were measured in each cell population by qRT-PCR and normalized to 1,000 *β-actin*. (B) Quantification of the total number of CD3+CD4+TLR2+ and CD3+CD8+TLR2+ cells from IL-10−/− were determined by flow cytometry 4 weeks post-infection. (C and D) IL-10−/− mice were sacrificed at 1 week time intervals and analyzed by flow cytometry for TLR2 expression on

CD3$^+$CD4$^+$ T cells (C) and CD3$^+$CD8$^+$ T cells (D). (E–F) SMARTA/TCRα$^{-/-}$/IL-10$^{-/-}$ mice were infected with *B. burgdorferi* for 4 weeks, after which popliteal and inguinal lymph nodes were collected for analysis of T cells and TLR2 expression. (E) Numbers in upper left corner of flow plots are %TLR2$^+$ cells. (F) The frequency and total number of CD3$^+$CD4$^+$TLR2$^+$ cells were determined by flow cytometry. (G–H) OT-I/Rag2$^{-/-}$/IL-10$^{-/-}$ mice were infected with *B. burgdorferi* for 4 weeks, after which popliteal and inguinal lymph nodes were collected for analysis of T cells and TLR2 expression. (G) Numbers in upper left corner of flow plots are %TLR2$^+$ cells. (H) Quantification of the frequency and total number of CD3$^+$CD8$^+$TLR2$^+$ cells were determined by flow cytometry. Error bars indicate the SEM (n 3 per group). Significant differences between infected and uninfected groups by Student's t-test are indicated (*p<0.05, **p<0.01, ***p<0.001 ****p<0.0001). Data are representative of two independent experiments.
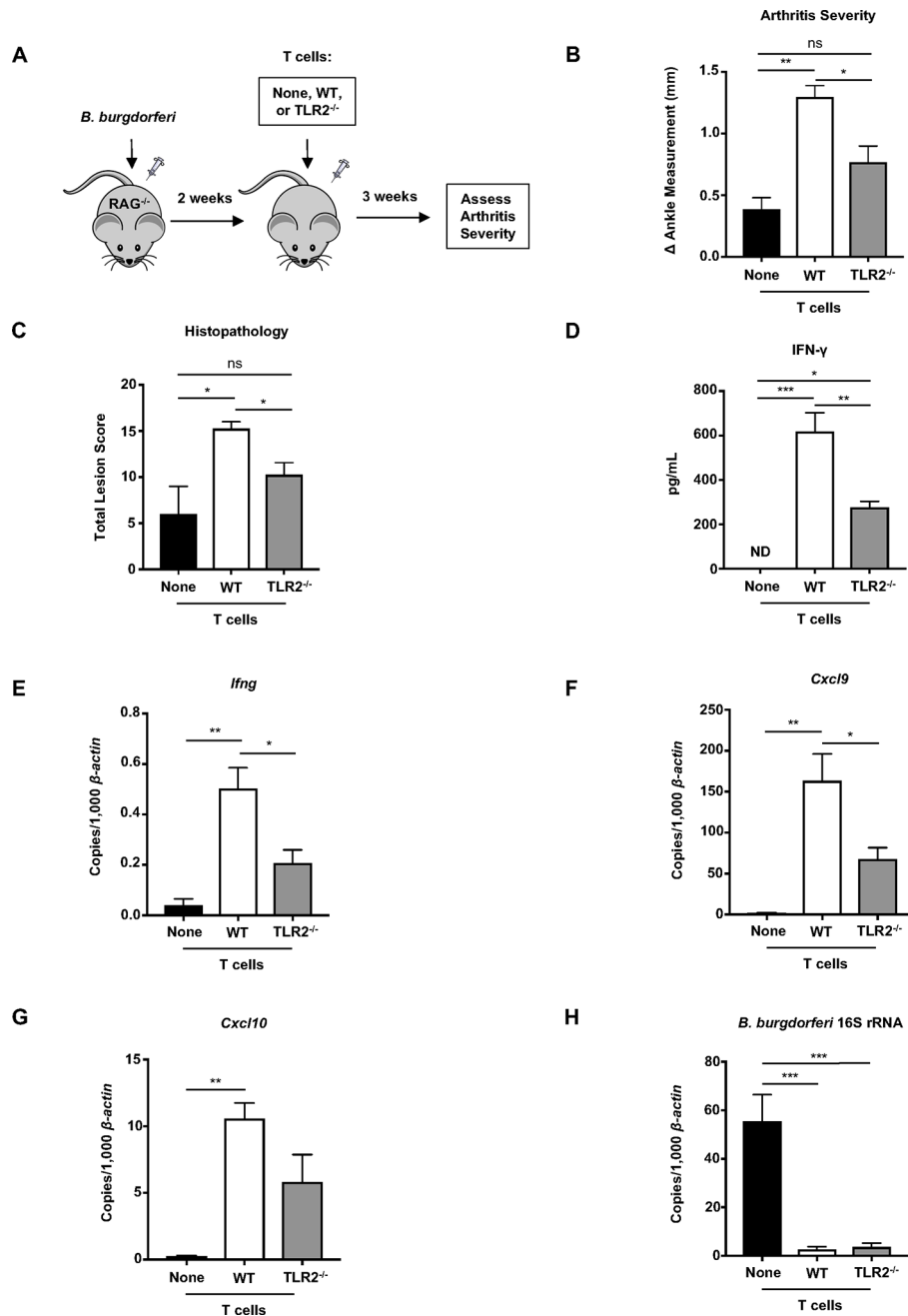
Figure 7. TLR2 expression on T cells enhances IFN-γ production and Lyme arthritis

(A) C57BL/6 Rag1$^{-/-}$ mice were infected with *B. burgdorferi* 2 weeks before an intravenous injection of 6.5×10^6 T cells isolated from the popliteal and inguinal lymph nodes and spleens of naïve healthy C57BL/6 WT or TLR2$^{-/-}$ mice. Infected Rag1$^{-/-}$ mice that did not receive lymphocytes served as controls. (B) Arthritis severity was determined 5 weeks post infection (3 weeks after injection of T cells). (C) The most swollen ankle was assessed by histopathologic evaluation in a blind fashion. Scores 0–5, with 5 being most severe, were assigned to each sample. The total score is shown is based on polymorphic (neutrophils) and/or mononuclear cell (lymphocyte/macrophage) infiltrates, tendon sheath thickness, and

reactive/reparative responses affecting the joint. (D) Quantification of IFN-γ in the serum was determined using ELISA. (E–H) Quantification of *Ifng*, *Cxcl9*, *Cxcl10*, and *B. burgdorferi*-specific *16S rRNA* was normalized to 1,000 *β-actin* in the joint using qRT-PCR. Error bars indicate the SEM (n = 4 per group). Statistically significant differences between groups by ANOVA followed by Bonferroni's post-hoc test is indicated (*p<0.05, **p<0.01, ***p<0.001). For lesion scoring, Mann-Whitney *U* test was used to determine whether there was statistically significant difference with groups, with p values indicated.

Table 1

Arthritis and inflammatory mediators are sustained for 18 weeks in joint tissue of *B. burgdorferi*-infected IL-10$^{-/-}$ mice

Mouse Genotype	Infection	Arthritis (mm)	Transcript/1,000 *β-actin*				
			Ifng	*Cxcl9*	*Cxcl10*	*Il10*	*B. burgdorferi 16s rRNA*
B6	Mock	0.01 ± 0.01	0.04 ± 0.02	3.70 ± 0.65	1.91 ± 058	ND	ND
	Bb	0.10 ± 0.04	0.05 ± 0.02	6.68 ± 1.21	1.94 ± 1.9	**0.08 ± 0.02**	**9.43 ± 4.90**
B6 IL-10$^{-/-}$	Mock	0.01 ± 0.01	0.06 ± 0.02	6.93 ± 1.53	1.80 ± 0.53	ND	ND
	Bb	**0.64 ± 0.5**	**2.12 ± 0.45**	**249 ± 45.18**	**21.14 ± 2.62**	ND	ND

B6 and IL-10$^{-/-}$ mice were infected with *B. burgdorferi* for 18 weeks, after which joints were harvested for analysis of inflammation and bacterial burden. Transcripts for *Ifng, Cxcl9, Cxcl10, Il10,* and *B. burgdorferi*-specific *16S rRNA* were measured by qRT-PCR and normalized to *β-actin.* Values for infected mice that are significantly different from mock-infected are indicated in **bold** ± SEM (n 3 per group), by Student's t test (p<0.01). ND = Not detected.